ATLAS searches for resonances decaying to Higgs boson pairs

Bill Balunas

University of Cambridge

9 November 2022

Why HH resonances?

In the SM, the Higgs field generally couples to every other field

– Exception: gauge fields under which it isn't charged (gluon, photon)

– $\Phi^\dagger\Phi$ is dimension-2 and a singlet under all SM symmetries

For a BSM theory with a new field X, it's difficult to avoid interactions with H

– Usually only a manually-inserted symmetry will prevent this.

– Example for boson X: $\mathcal{L}_{\text{int}} = g\Phi^\dagger\Phi X^\dagger X$ (plenty of other structures possible, depending on model)
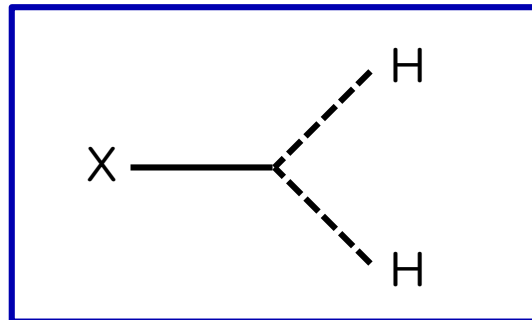
Interactions like this end up ubiquitous in BSM models

HH itself has many decay modes.
Which ones to search in?

– A complicated trade-off between
  signal rates, mass resolution,
  backgrounds, ease of triggering…

– It turns out that some of the best are
  bbγγ, bbττ, and bbbb. Today I'll
  present these.

– This doesn't mean all others are
  necessarily bad: we just don't currently
  have resonant results on them.

	bb	WW	ττ	ZZ	γγ
bb	34%				
WW	25%	4.6%			
ττ	7.3%	2.7%	0.39%		
ZZ	3.1%	1.1%	0.33%	0.069%	
γγ	0.26%	0.10%	0.028%	0.012%	0.0005%

Current status at ATLAS

A summary of ATLAS full Run 2 results on resonant di-Higgs production:

Decay channel	Reference	Release date
bbγγ	Phys. Rev. D 106 (2022) 052001	22 Dec 2021
bbττ	arXiv:2209.10910	22 Sep 2022
bbττ (merged ττ)	JHEP 11 (2020) 163	29 July 2020	← Not discussed today
bbbb	Phys. Rev. D 105 (2022) 092002	15 Feb 2022
Combination	ATLAS-CONF-2021-052	16 Oct 2021

We also have several results on non-resonant di-Higgs production

- Some included in these papers

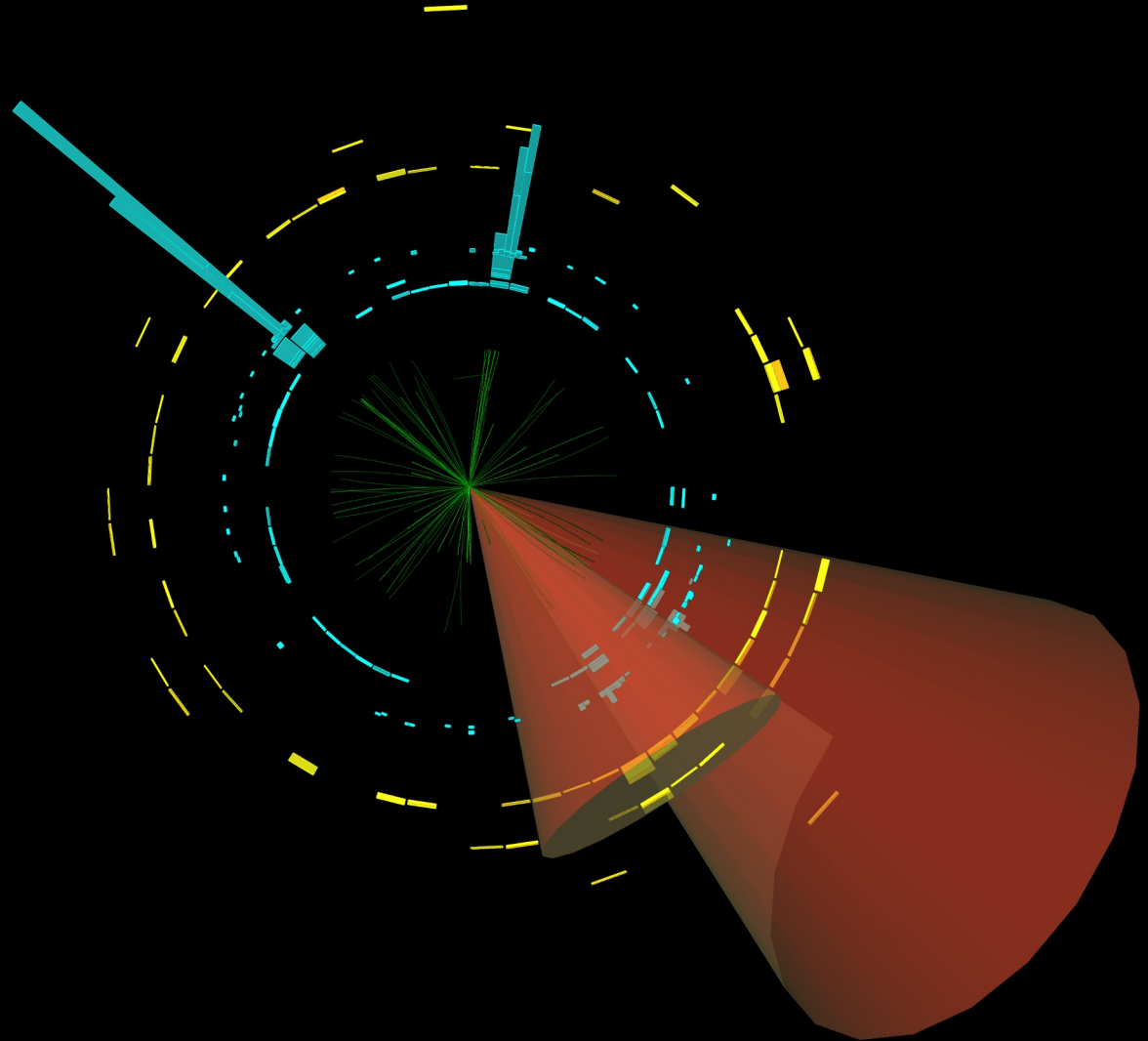- Jason Veatch will cover these in his talk later this session

HH→bbγγ

ATLAS
EXPERIMENT

Run: 329964
Event: 796155578
2017-07-17 23:58:15 CEST

HH→bbγγ: Overview

The bbγγ final state is very clean, but has low branching fraction (~0.26% in SM)

- Very statistically limited, and will remain so for a long time to come

- Photon triggers allow good reach to low masses

- We cover resonance masses up to 1 TeV with this channel

Method: Use two BDTs to cut away background, then fit the $m_{\gamma\gamma}$ distribution

- One to discriminate vs. H→γγ and one to discriminate vs. everything else (smooth $m_{\gamma\gamma}$)

- Each BDT is trained across all signal masses, reweighted to remove bias.

  - Different cut values optimized for each signal mass.

- Input features are a broad set of kinematic variables: momenta, masses, angles (but not $m_{\gamma\gamma}$)

HH→bbγγ: Background modelling

H→γγ background **taken from MC simulation**

- Fit $m_{\gamma\gamma}$ distribution to a double-sided Crystal Ball to smooth stat fluctuations
- ZH and ttH contributions are dominant

**"Continuum" γγ background** **modeled as an exponential function** in $m_{\gamma\gamma}$

- Limited stats mean this is sufficient despite its simplicity
- Potential bias ("spurious signal") accounted for with systematic uncertainties

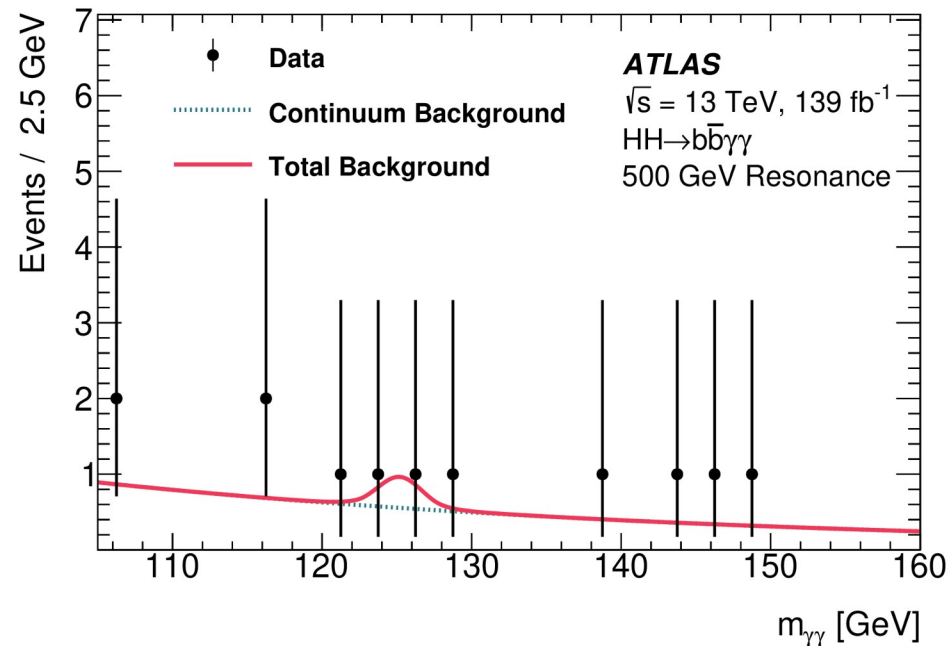**This procedure is repeated for every signal mass hypothesis**

- Different BDT optimization means different events are selected in each case

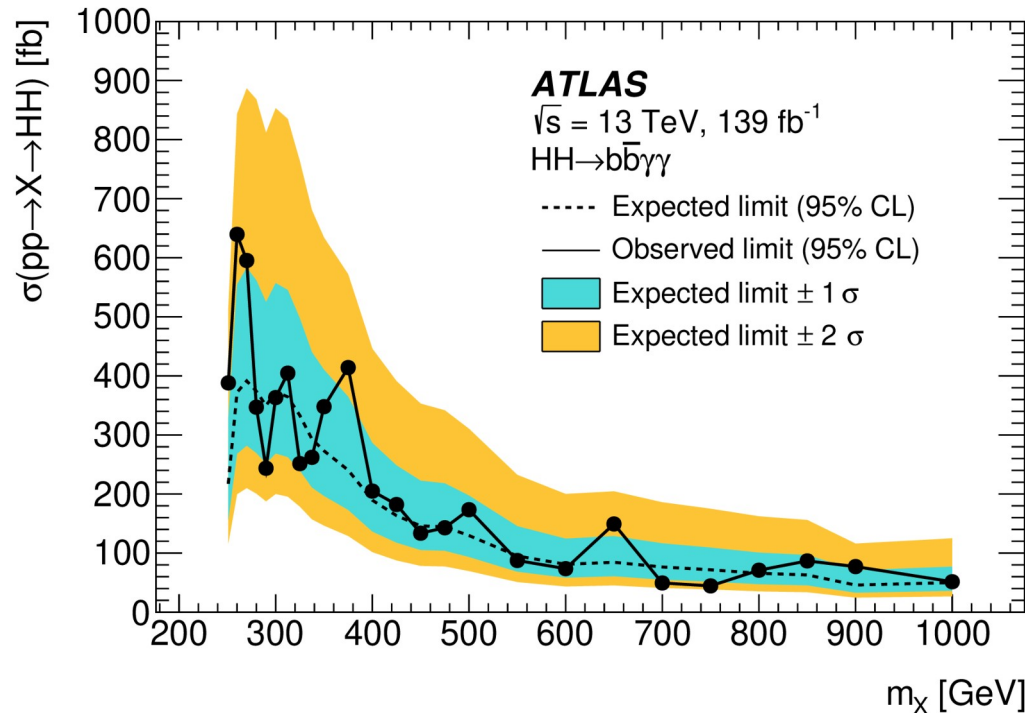# HH→bbγγ: Results

Data are consistent with the background model.
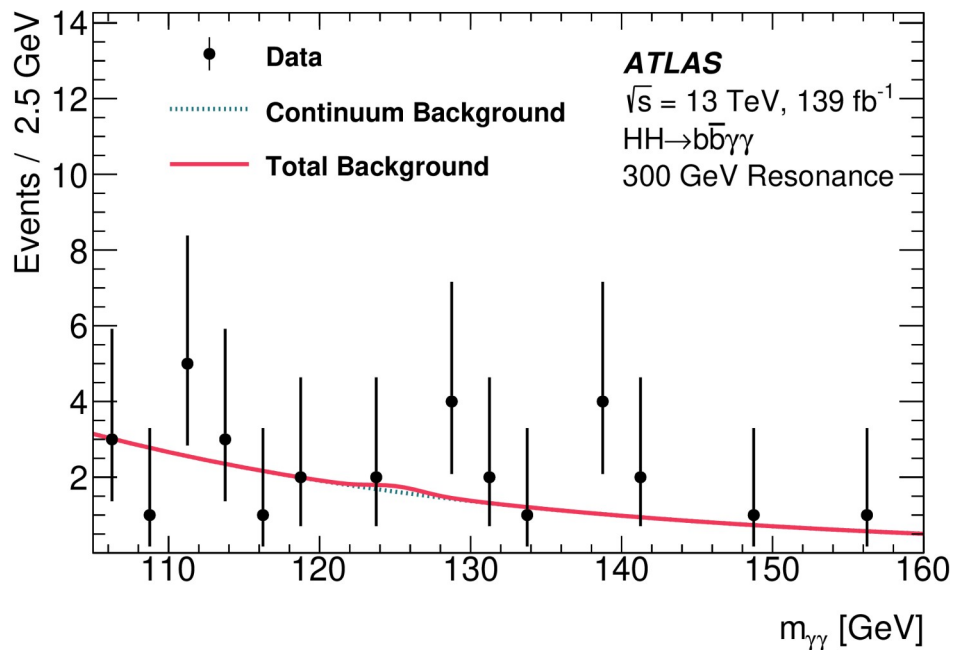
300 GeV selection

500 GeV selection

HH→bbγγ: Results
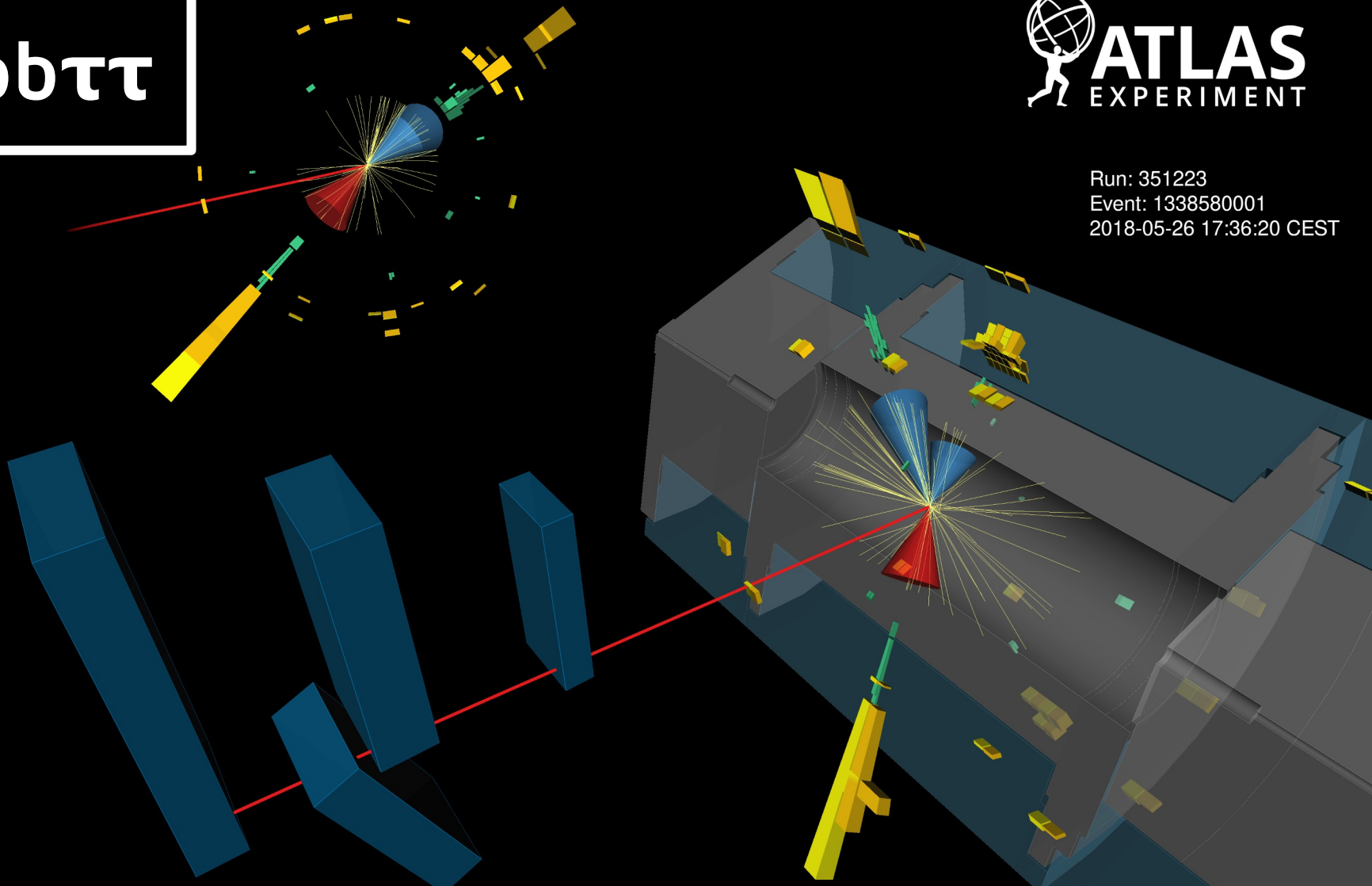
Set cross section limits using narrow scalar resonance as benchmark

Statistical uncertainties dominate the sensitivity by a wide margin

HH→bbττ

ATLAS
EXPERIMENT

Run: 351223
Event: 1338580001
2018-05-26 17:36:20 CEST

HH→bbττ: Overview

Higher branching fraction (~7.3% in SM) than bbγγ, but **bigger and more complex backgrounds**

- We consider the semi-leptonic ($\tau_{lep}\tau_{had}$) and fully-hadronic ($\tau_{had}\tau_{had}$) cases in this search.

- Resonance masses up to 1.6 TeV covered here

Method: **Select signal-like events using object-based cuts, then use a neural network (NN) to construct a discriminant, which we then fit.**

- NN input features are kinematic variables (momenta, masses, angles)*

- NN is parameterized on m_{HH} for optimal performance across the whole range

Complex trigger strategy using a mixture of hadronic single-/di-τ triggers and lepton/lepton+τ triggers

- Separate event categories constructed according to these, as background composition varies

* Full list in backup slides

HH→bbττ: Background modelling

Backgrounds are estimated using a mix of simulation and control samples in data:

- Top with real τ_{had}: Use MC simulation

- Top/multijet with fake τ_{had}: Use a "fake factor" method to extrapolate from control regions
  - See paper for details, but broadly this involves inverting the τ ID and/or other cuts for samples enriched in "fakes"

- Z + heavy flavor: Use MC simulation, but correct it using a data control region with Z → ll selection

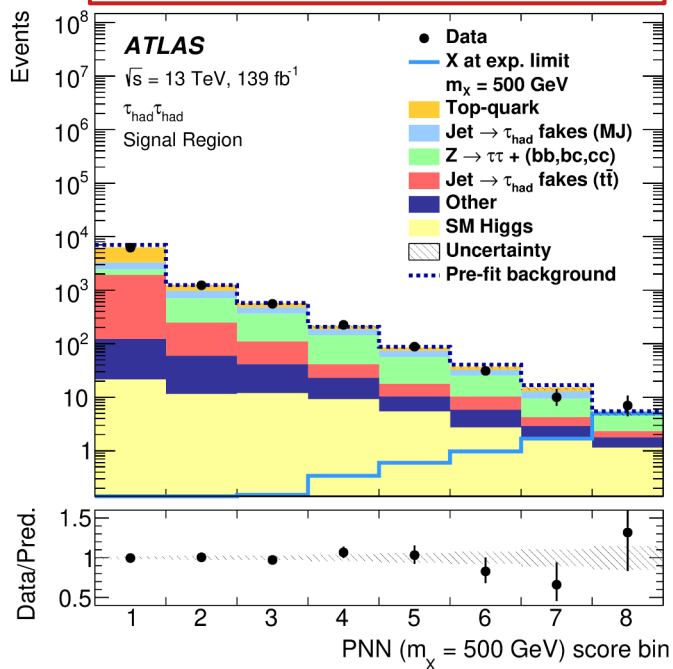- Other small backgrounds (single Higgs, diboson, etc.): Use MC simulation
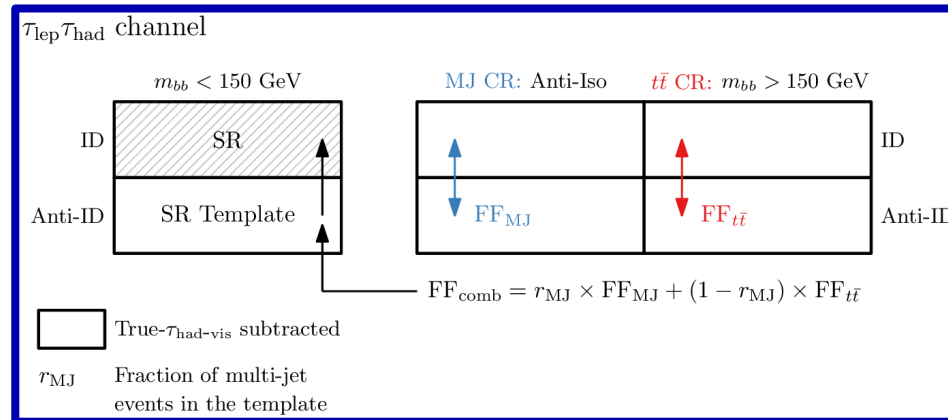
Example: fake τ_{had} estimation scheme for semi-leptonic channel

HH→bbττ: Results

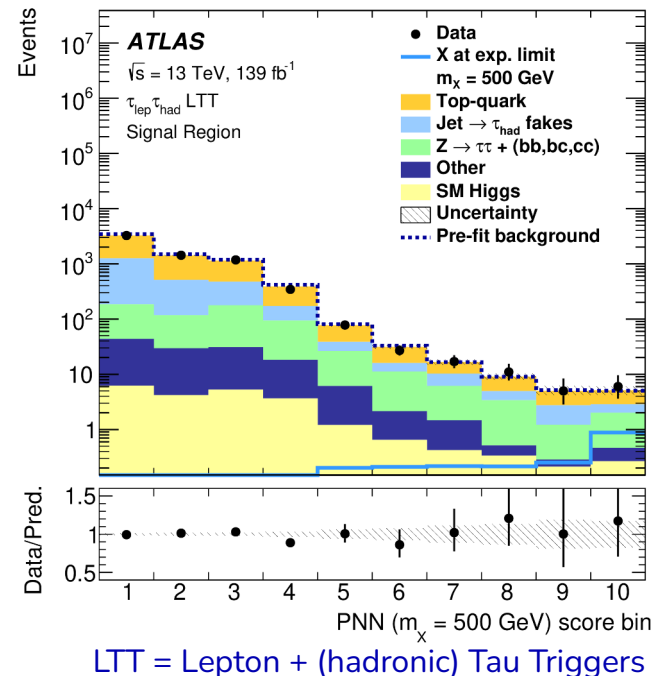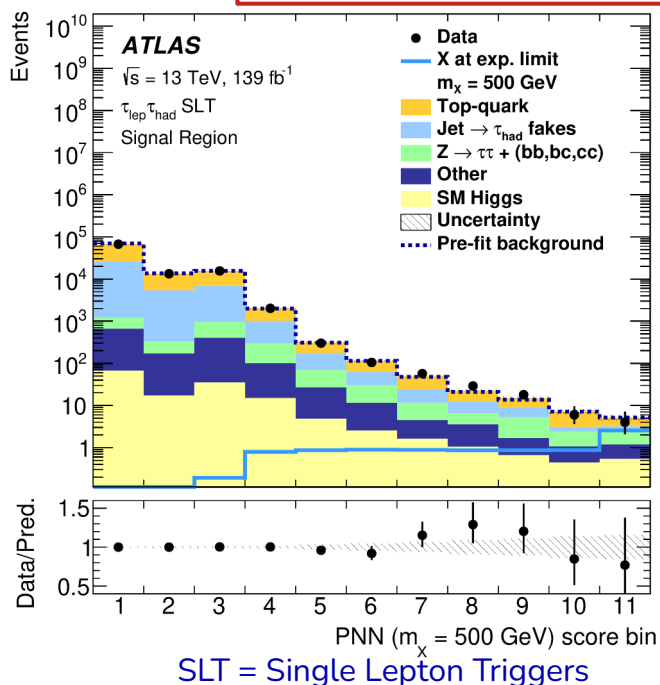## Data are consistent with the background model.

– Example below shows the 500 GeV signal mass hypothesis

Fully Hadronic   **Semi-leptonic**
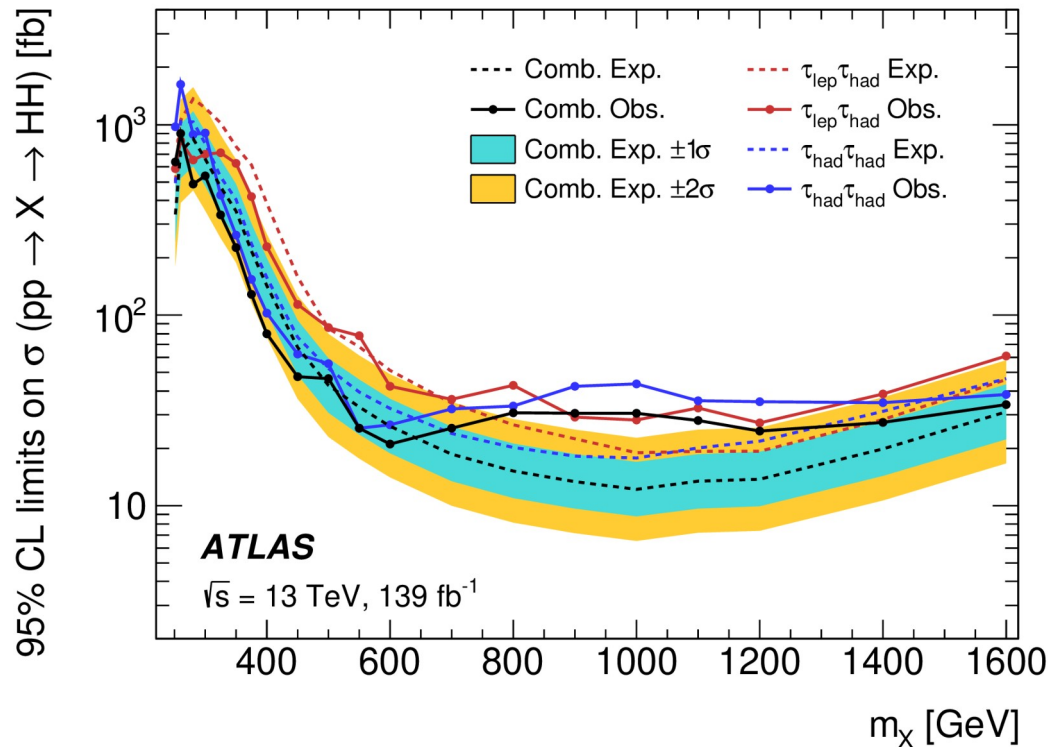
SLT = Single Lepton Triggers   LTT = Lepton + (hadronic) Tau Triggers

HH→bbττ: Results

Set cross section limits (same narrow scalar resonance benchmark as bbγγ)

Comparable sensitivity between $\tau_{lep}\tau_{had}$ and $\tau_{had}\tau_{had}$

Statistical uncertainties dominate the sensitivity (but systematics not quite negligible)

Excess at ~1 TeV has a global significance of **2.0σ**

ATLAS
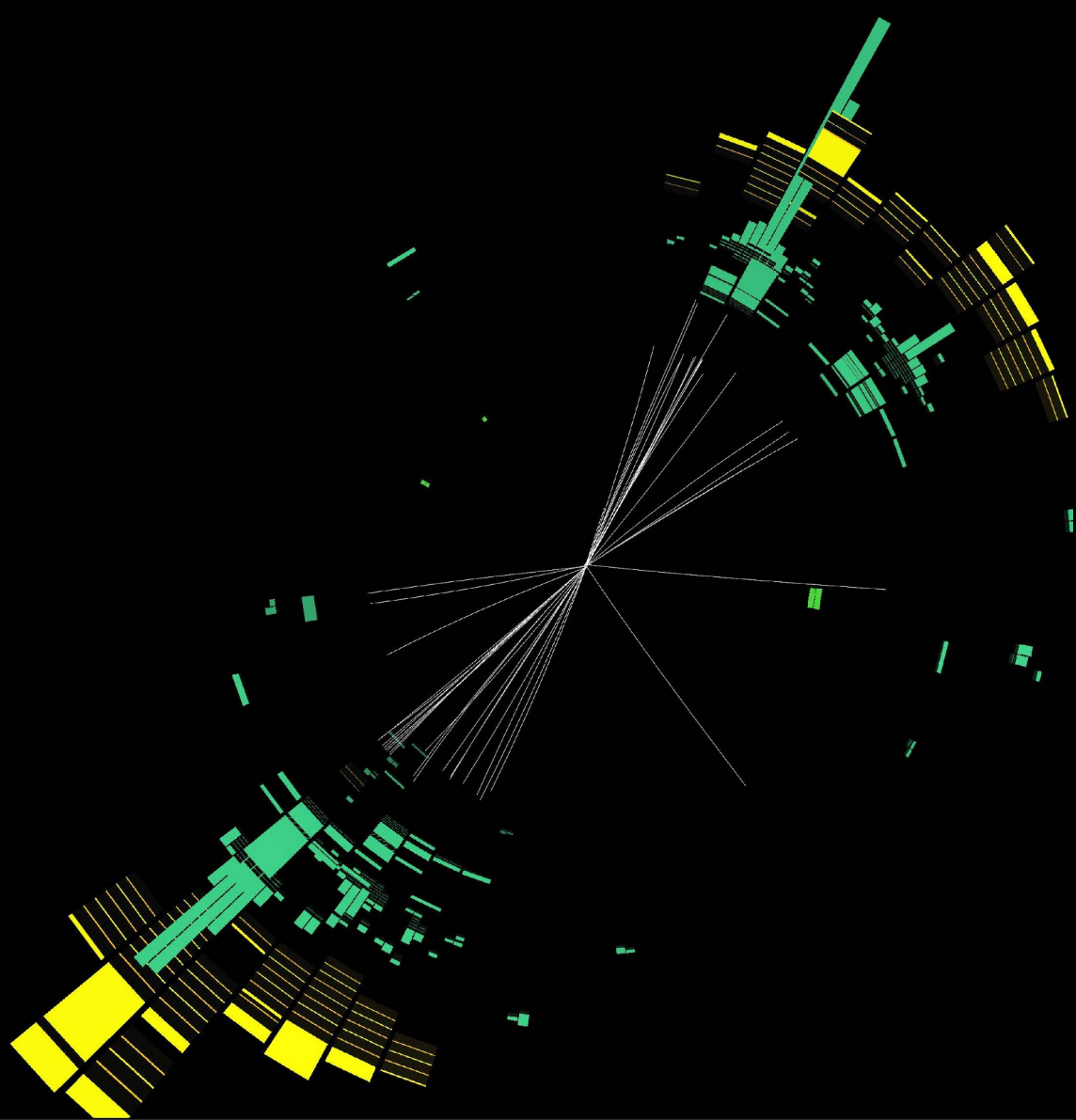EXPERIMENT

Run: 356259
Event: 311347503
2018-07-22 20:00:32 CEST

HH→bbbb
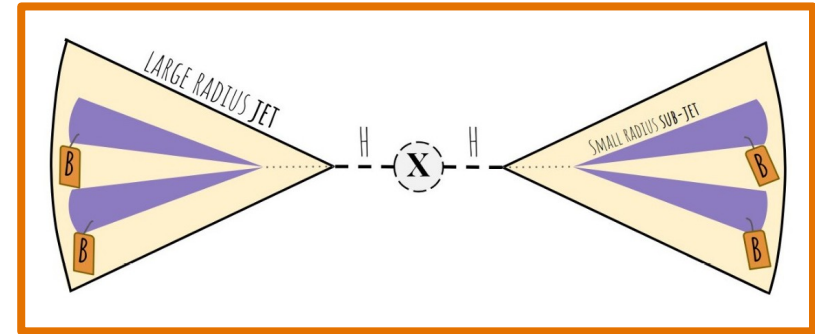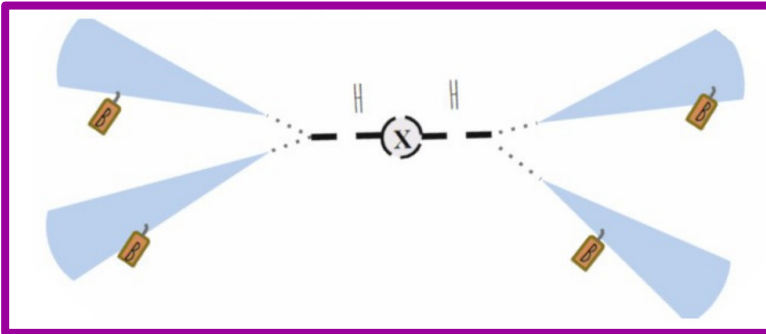
HH→bbbb: Overview

bbbb **has the** **highest branching fraction** **(~34% in SM), but the** **largest background**

– QCD cross sections are big, even for 4 jets after b-tagging requirements!

Depending on the resonance mass, the detector signature can be **4 "resolved" jets** **or** **2 merged ("boosted") ones.**

– We treat both cases at ATLAS, for mass coverage up to **5 TeV**.

HH→bbbb: Resolved Strategy

1. Select events with 4 b-tagged jets* (p_T >40 GeV, so we can trigger on them)

2. Pair these jets into 2 Higgs boson candidates

– Boosted decision tree trained on simulated signal to distinguish correct pairs from incorrect ones

– **Input variables:** angles between the jets. Parameterized on the 4-jet invariant mass

3. Construct a signal region based on the *H* candidate masses

– Also construct adjacent "control" and "validation" regions for estimating background

4. Construct background model and fit m_{HH} spectrum to search for a resonant bump
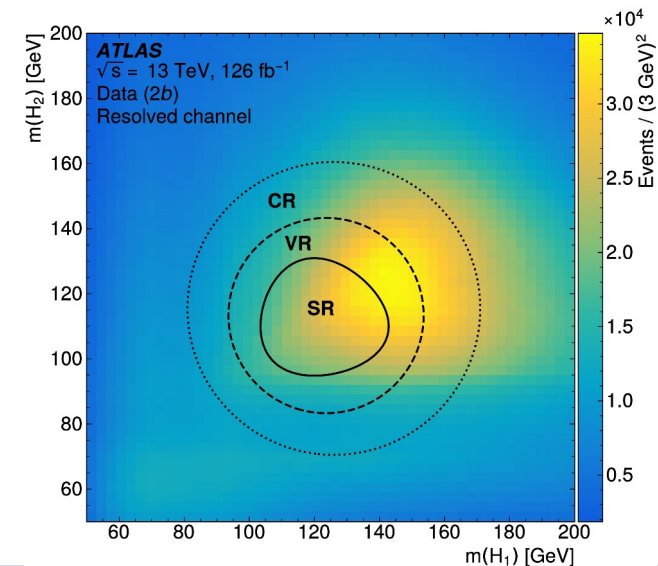
*Anti-k_t clustering, R=0.4, Particle Flow inputs. 77% eff. b-tagging WP

HH→bbbb: Boosted Strategy

1. Select events with 2 large-R jets* (one with $p_T > 450$ GeV, so we can trigger on it)

2. b-tag them using variable-radius subjets constructed from their associated tracks

– At very high resonance masses, even these get merged. Therefore, also keep events with only 2 or 3 b-tagged subjets in their own separate categories.

3... The rest of the procedure follows the resolved strategy closely
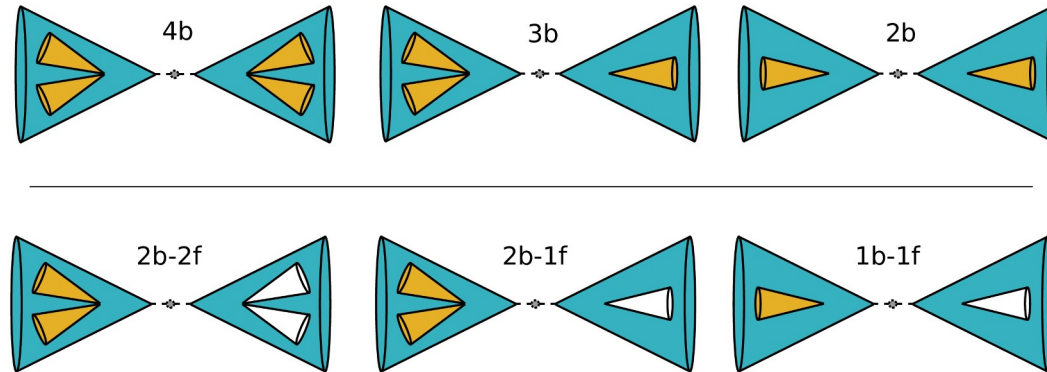
"Low-tag" control samples for background modeling

*Anti-k_t clustering, R=1.0, locally-calibrated calorimeter cluster inputs, trimmed (R=0.2, 5% threshold)

HH→bbbb: Background modelling

Background is overwhelmingly pure QCD. Can't model with simulation!

– Use a data-driven method using a control sample with fewer b-tags (QCD is flavor-blind)

– Top pair background is nontrivial (5-10%) in the boosted channel, so MC is used for that.

Use the control regions to derive an extrapolation from low-tag to high-tag regions. Apply this to low-tag signal region equivalent.

– Resolved: Neural network with jet kinematic inputs is used to derive reweighting

– Boosted: High-tag/low-tag ratios of kinematic variables are fit with splines

– Check CR closure and accuracy in VR to estimate uncertainties on this extrapolation

HH→bbbb: Results

Data consistent with background.
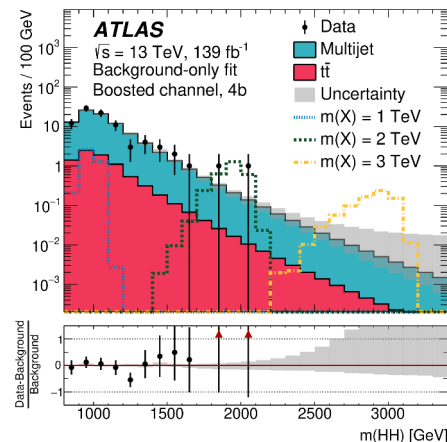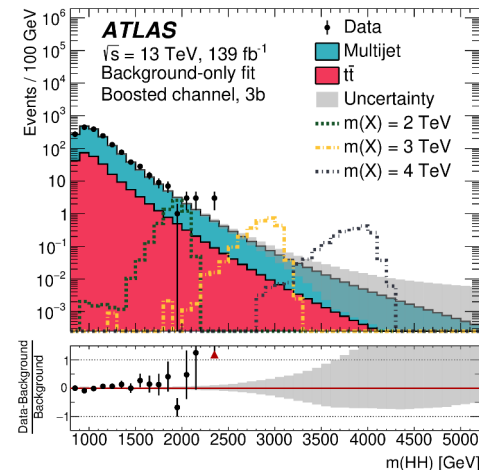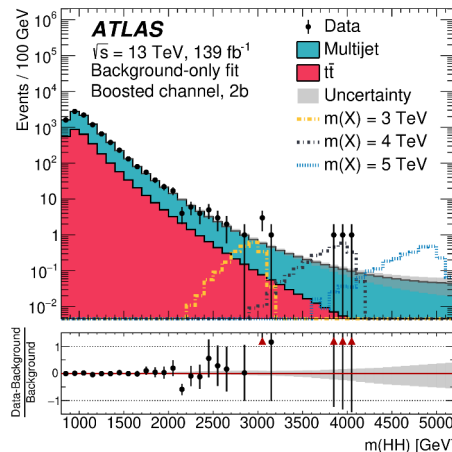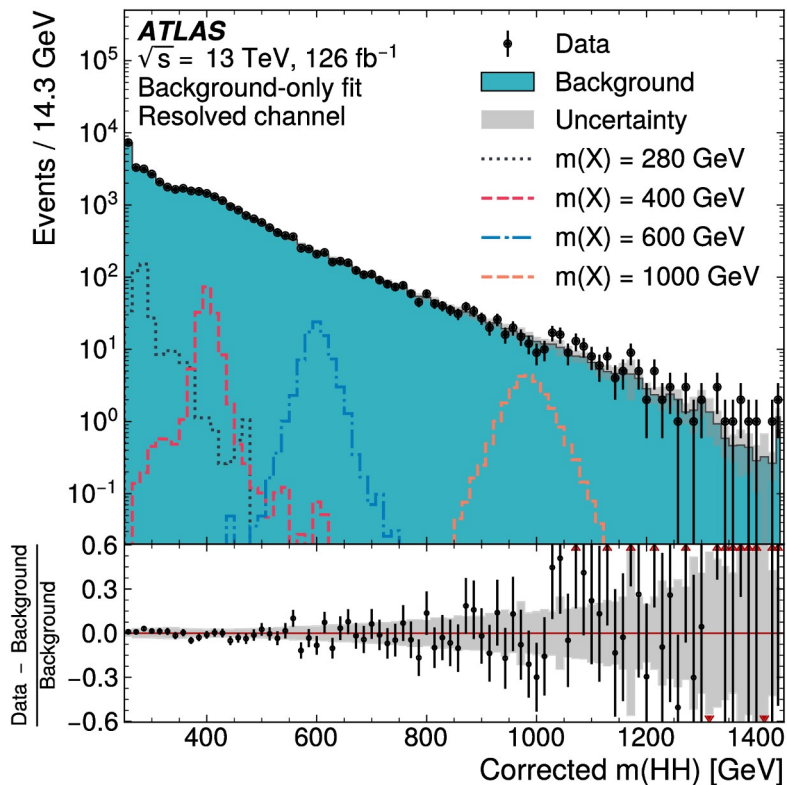
HH→bbbb: Results

Set cross section limits on benchmark models: generic narrow scalar produced in ggF, and RS graviton
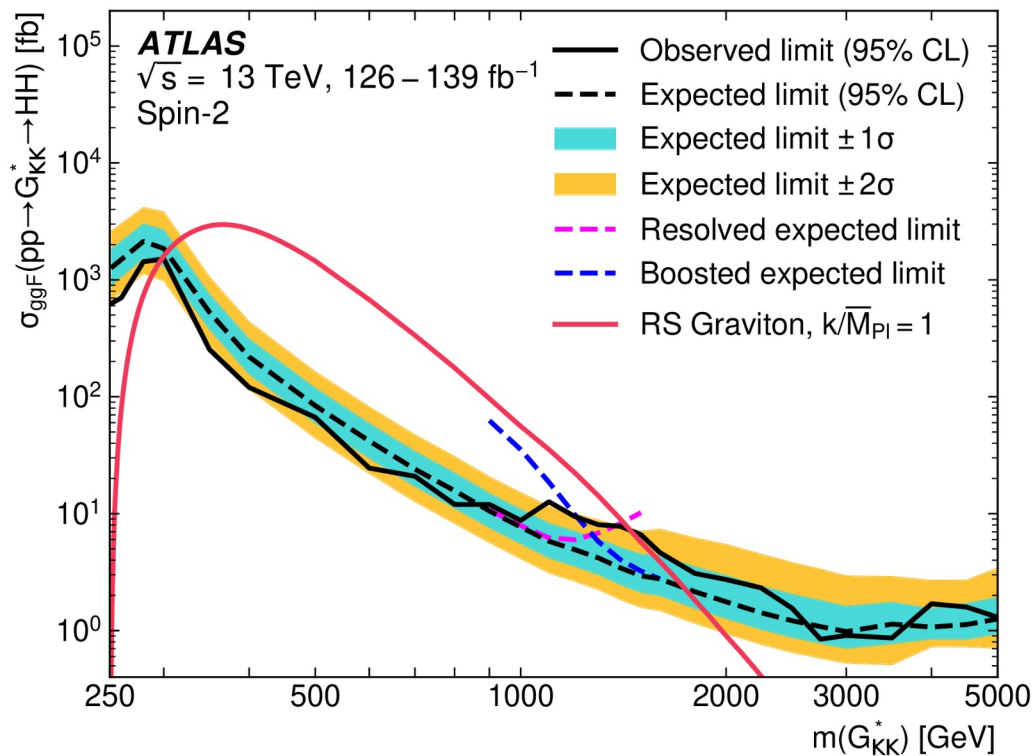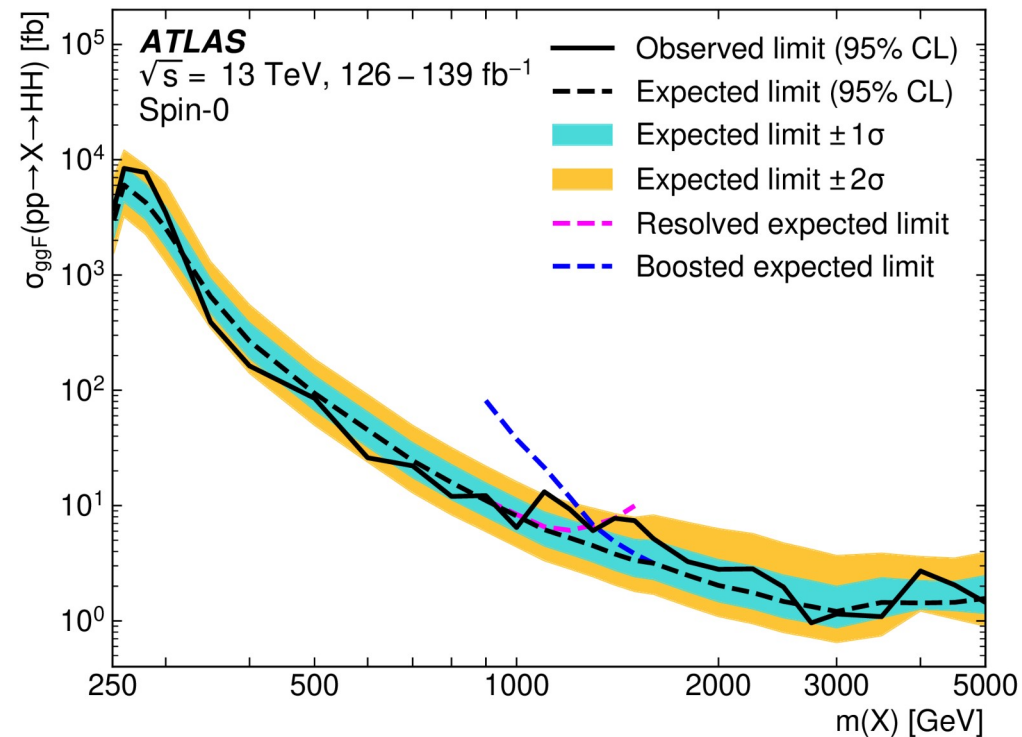
Dominant uncertainties are statistical in origin, even at low mass.

The big picture

We've continued to tighten constraints on HH resonances
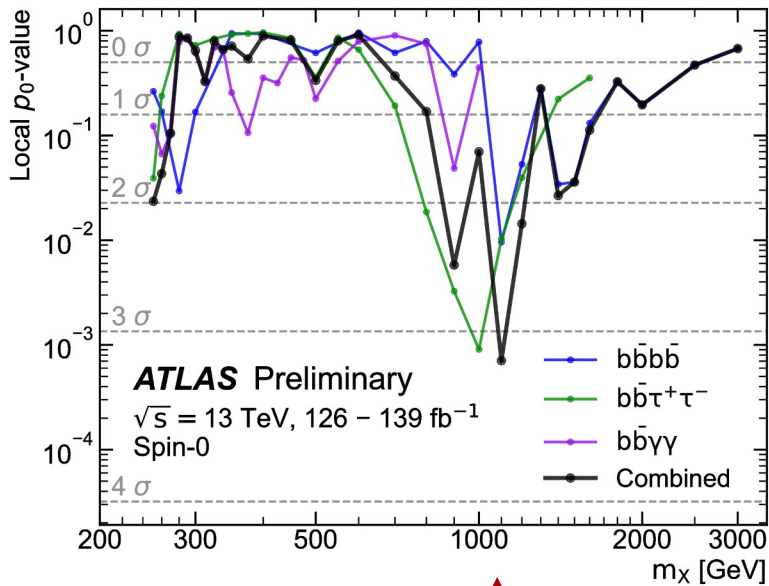
Global significance of largest excess is **2.1σ**
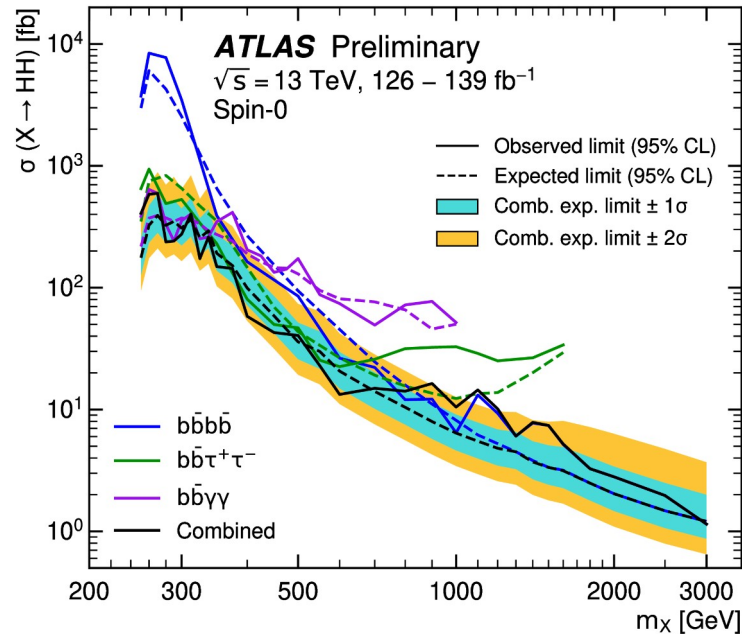
Each of the 3 decay channels is the most sensitive in a different mass range: **good complementarity**

Summary

ATLAS has searched for HH resonances with the full Run 2 dataset in the bbγγ, bbττ, and bbbb channels

- Data are consistent with the Standard Model in all cases

- Largest excess is 2.1σ (global) at 1 TeV

All channels are statistically-limited, especially at high mass

- This doesn't mean waiting for more data is the only thing to do!

- Ways to reduce background (e.g. better mass resolution or b-tagging discrimination) will always bring improvements. Performance work is crucial to our success!

With Run 3 underway, we're looking forward to doing this better than ever!

Backup

HH→bbγγ: Event selection

Quality & isolation

On top of the trigger requirements, events are selected if:

- At least two photons satisfy the object selection criteria detailed in Section 4.1.

- The diphoton invariant mass, built with the two leading photons, satisfies $105 < m_{\gamma\gamma} < 160$ GeV.

- The leading (subleading) photon p_T is larger than 35% (25%) of the mass of the diphoton system.

- Exactly two b-tagged jets are present. In order to remain statistically independent of the ATLAS search for $HH \to b\bar{b}b\bar{b}$ [105], any event with more than two b-jets passing the 77% efficient working point is rejected.

- No electrons or muons are present.

- Fewer than six central ($|\eta| < 2.5$) jets are present. This helps to reject $t\bar{t}H$ events where the top quarks decay hadronically.

HH→bbγγ: BDT input variables

Variable	Definition
Photon-related kinematic variables	
$p_{\mathrm{T}}^{\gamma\gamma}$, $y^{\gamma\gamma}$	Transverse momentum and rapidity of the diphoton system
$\Delta\phi_{\gamma\gamma}$ and $\Delta R_{\gamma\gamma}$	Azimuthal angle and ΔR between the two photons
Jet-related kinematic variables	
$m_{b\bar{b}}$, $p_{\mathrm{T}}^{b\bar{b}}$ and $y_{b\bar{b}}$	Invariant mass, transverse momentum and rapidity of the b-tagged jets system
$\Delta\phi_{b\bar{b}}$ and $\Delta R_{b\bar{b}}$	Azimuthal angle and ΔR between the two b-tagged jets
N_{jets} and $N_{b\text{-jets}}$	Number of jets and number of b-tagged jets
H_{T}	Scalar sum of the p_{T} of the jets in the event
Diphoton+dijet-related kinematic variables	
$m_{b\bar{b}\gamma\gamma}^{*}$	Invariant mass of the diphoton plus b-tagged jets system
$\Delta y_{\gamma\gamma,b\bar{b}}$, $\Delta\phi_{\gamma\gamma,b\bar{b}}$ and $\Delta R_{\gamma\gamma,b\bar{b}}$	Distance in rapidity, azimuthal angle and ΔR between the diphoton and the b-tagged jets system
Missing transverse momentum variables	
$E_{\mathrm{T}}^{\mathrm{miss}}$	Missing transverse momentum

Table 8: Breakdown of the dominant systematic uncertainties. The impact of the uncertainties corresponds to the relative variation of the expected upper limit on the cross section when re-evaluating the profile likelihood ratio after fixing the nuisance parameter in question to its best-fit value, while all remaining nuisance parameters remain free to float. The impact is shown in %. Only systematic uncertainties with an impact of at least 0.2% are shown. Uncertainties of the "Norm. + Shape" type affect both the normalization and the parameters of the functional form. The rest of the uncertainties affect only the yields.

		Relative impact of the systematic uncertainties [%]	
Source	Type	Nonresonant analysis HH	Resonant analysis $m_X = 300$ GeV
Experimental			
Photon energy resolution	Norm. + Shape	0.4	0.6
Jet energy scale and resolution	Normalization	< 0.2	0.3
Flavor tagging	Normalization	< 0.2	0.2
Theoretical			
Factorization and renormalization scale	Normalization	0.3	< 0.2
Parton showering model	Norm. + Shape	0.6	2.6
Heavy-flavor content	Normalization	0.3	< 0.2
$\mathcal{B}(H \to \gamma\gamma, b\bar{b})$	Normalization	0.2	< 0.2
Spurious signal	Normalization	3.0	3.3

No substantive changes to methodology. **We've made a few minor improvements and made more information available:**

- Updated parton shower uncertainties on signal to more precise estimate

- Updated to newer, improved b-tagging calibration

- Added calculation of global significance for largest excess

- Updated validation region plots with dedicated systematic uncertainties

- Added further supplementary material on the fake tau background estimate and systematic uncertainty effects

$\tau_{\text{had}}\tau_{\text{had}}$ category		$\tau_{\text{lep}}\tau_{\text{had}}$ categories	
STT	DTT	SLT	LTT

e/μ selection

No loose e/μ

Exactly one loose e/μ
e (μ) must be tight (medium and have $|\eta| < 2.5$)

| | | $p_T^e > 25, 27$ GeV | 18 GeV $< p_T^e <$ SLT cut |
| | | $p_T^\mu > 21, 27$ GeV | 15 GeV $< p_T^\mu <$ SLT cut |

$\tau_{\text{had-vis}}$ selection

Two loose $\tau_{\text{had-vis}}$

One loose $\tau_{\text{had-vis}}$
$|\eta| < 2.3$

$p_T >$ 100, 140, 180 (25) GeV	$p_T > 40$ (30) GeV		$p_T > 30$ GeV

Jet selection

≥ 2 jets with $|\eta| < 2.5$

Leading jet $p_T > 45$ GeV	Trigger dependent	Leading jet $p_T > 45$ GeV	Trigger dependent

Event-level selection

Trigger requirements passed

Collision vertex reconstructed

$m_{\tau\tau}^{\text{MMC}} > 60$ GeV

Opposite-sign electric charges of $e/\mu/\tau_{\text{had-vis}}$ and $\tau_{\text{had-vis}}$
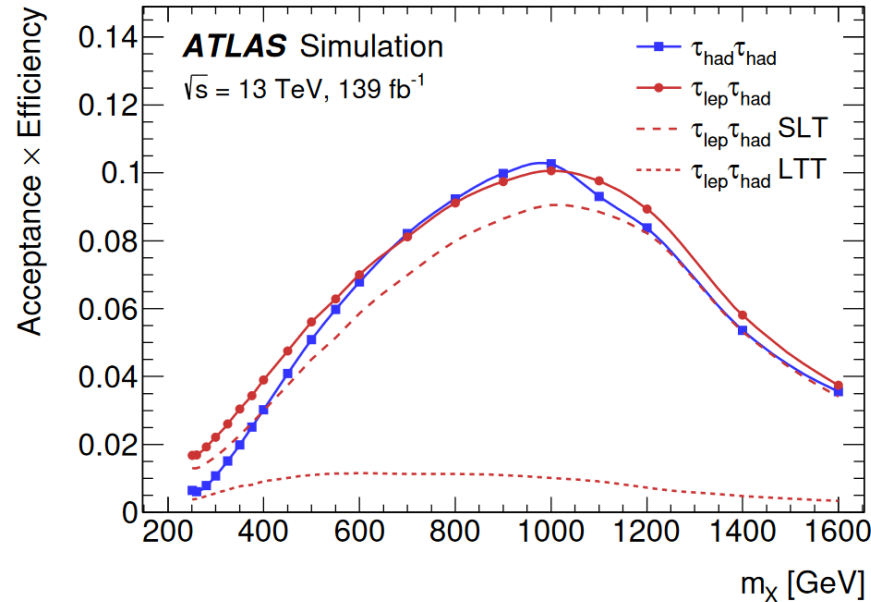
Exactly two b-tagged jets

$m_{bb} < 150$ GeV

Figure 2: Acceptance times efficiency for the full analysis selections as a function of the resonance mass m_X in the $\tau_{had}\tau_{had}$, $\tau_{lep}\tau_{had}$ SLT and $\tau_{lep}\tau_{had}$ LTT trigger categories, shown in solid line with square markers, dashed and dotted lines, respectively. The solid line with circle markers is the acceptance times efficiency curve for the combined $\tau_{lep}\tau_{had}$ category. The acceptance times efficiency for $X \to HH \to b\bar{b}\tau^+\tau^-$ decays is evaluated with respect to the targeted τ-lepton pair decay mode ($\tau_{lep}\tau_{had}$ or $\tau_{had}\tau_{had}$).

Variable	$\tau_{\mathrm{had}}\tau_{\mathrm{had}}$	$\tau_{\mathrm{lep}}\tau_{\mathrm{had}}$ SLT	$\tau_{\mathrm{lep}}\tau_{\mathrm{had}}$ LTT
m_{HH}	✓	✓	✓
$m_{\tau\tau}^{\mathrm{MMC}}$	✓	✓	✓
m_{bb}	✓	✓	✓
$\Delta R(\tau, \tau)$	✓	✓	✓
$\Delta R(b, b)$	✓	✓	
$\Delta p_{\mathrm{T}}(\ell, \tau)$		✓	✓
Sub-leading b-tagged jet p_{T}		✓	
m_{T}^{W}		✓	
$E_{\mathrm{T}}^{\mathrm{miss}}$		✓	
$\mathbf{p}_{\mathrm{T}}^{\mathrm{miss}}\ \phi$ centrality		✓	
$\Delta\phi(\ell\tau, bb)$		✓	
$\Delta\phi(\ell, \mathbf{p}_{\mathrm{T}}^{\mathrm{miss}})$			✓
$\Delta\phi(\tau\tau, \mathbf{p}_{\mathrm{T}}^{\mathrm{miss}})$			✓
S_{T}			✓

HH→bbττ: Signal mass resolution
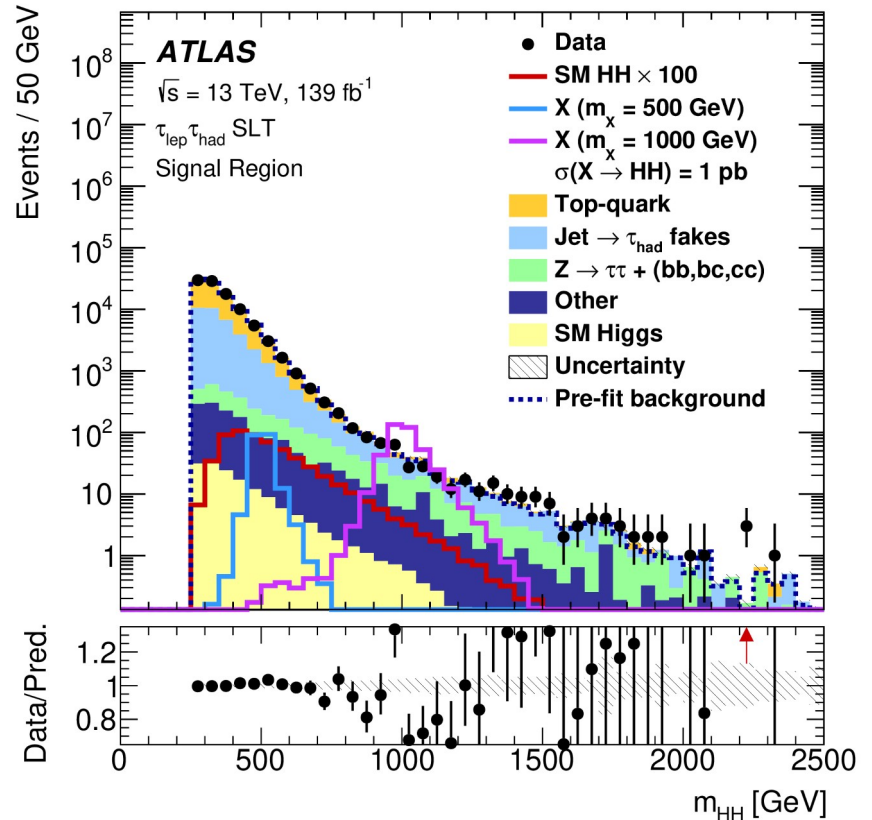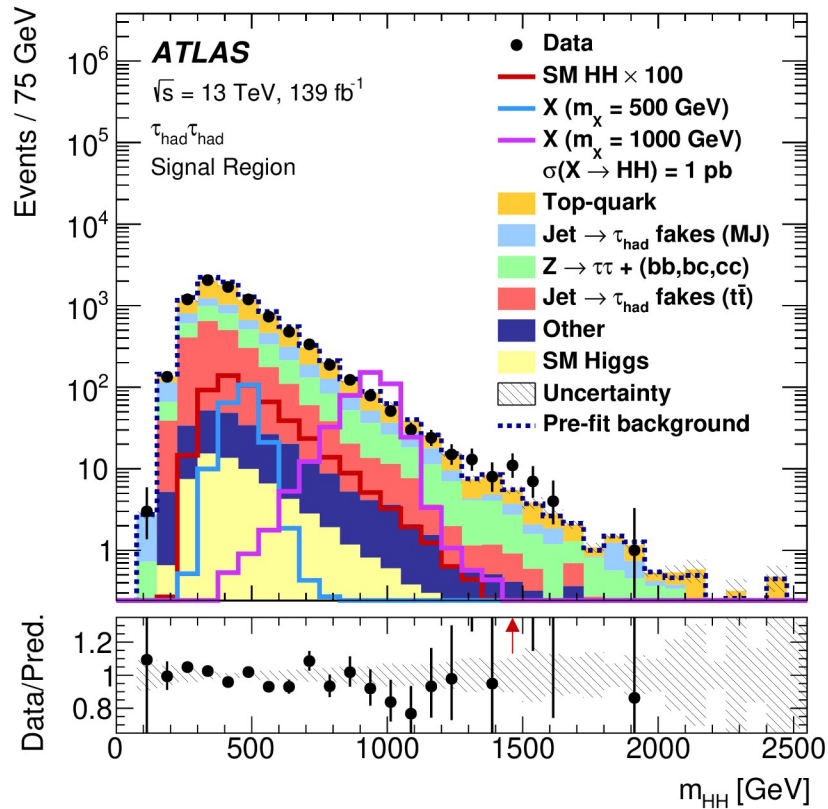
N.B. These signals are overlaid on the non-resonant background model

Table 4: Breakdown of the relative contributions to the uncertainty in the extracted signal cross-sections, as determined in the likelihood fit (described in Section 8) to data. They are obtained by fixing the relevant nuisance parameters in the likelihood fit, subtracting the square of the obtained uncertainty in the fitted signal cross-section from the square of the total uncertainty, taking the square root, and then dividing by the total uncertainty. The sum in quadrature of the individual components differs from the total uncertainty due to correlations between uncertainties in the different groups.

| Uncertainty source	Non-resonant HH	Resonant $X \to HH$		
		300 GeV	500 GeV	1000 GeV
Data statistical + floating normalisation	81%	76%	90%	93%
Data statistical	81%	76%	90%	93%
$t\bar{t}$ and Z + HF normalisations	4%	8%	3%	5%
Systematic	58%	65%	43%	37%
MC statistical	28%	44%	33%	18%
Experimental	12%	31%	8%	12%
Jet and $E_\mathrm{T}^\mathrm{miss}$	8%	27%	5%	4%
b-jet tagging	5%	5%	3%	7%
$\tau_\mathrm{had\text{-}vis}$	6%	12%	3%	8%
Electrons and muons	3%	3%	2%	2%
Luminosity and pile-up	3%	2%	2%	5%
Background and signal and modelling	42%	39%	26%	30%
Fake-$\tau_\mathrm{had\text{-}vis}$	8%	19%	4%	8%
Top-quark	24%	17%	12%	8%
$Z(\to \tau\tau)$ + HF	9%	17%	9%	15%
Single Higgs boson	29%	2%	14%	15%
Other backgrounds	3%	2%	5%	3%
Signal	5%	14%	7%	15%

HH→bbbb: Signal acceptance
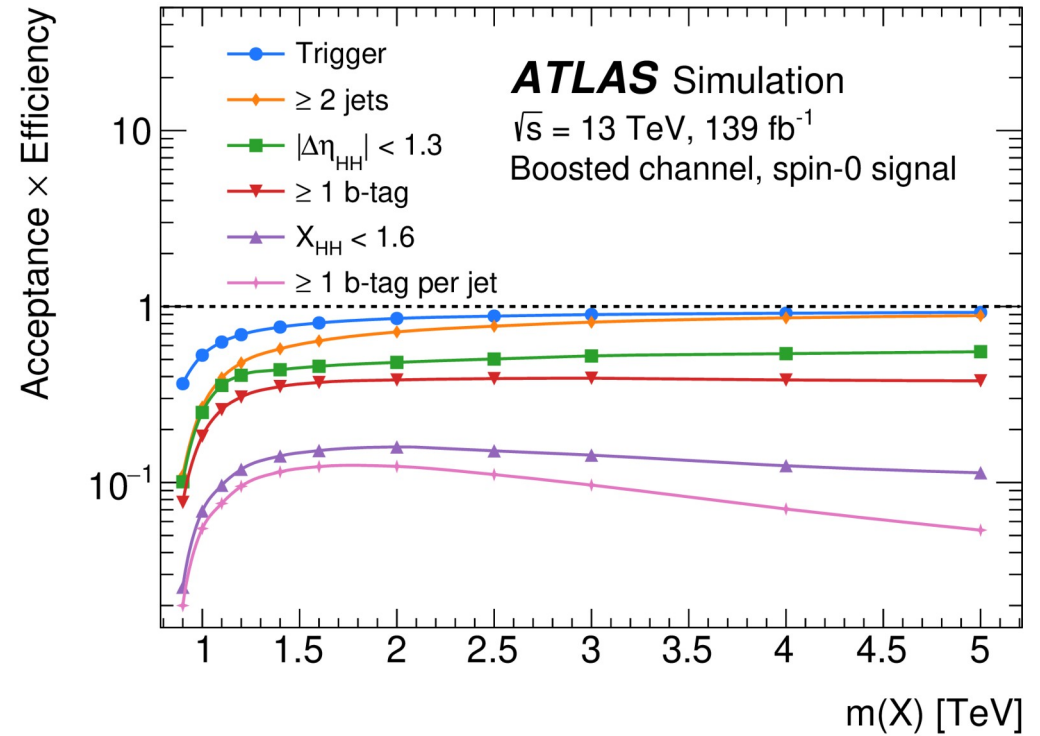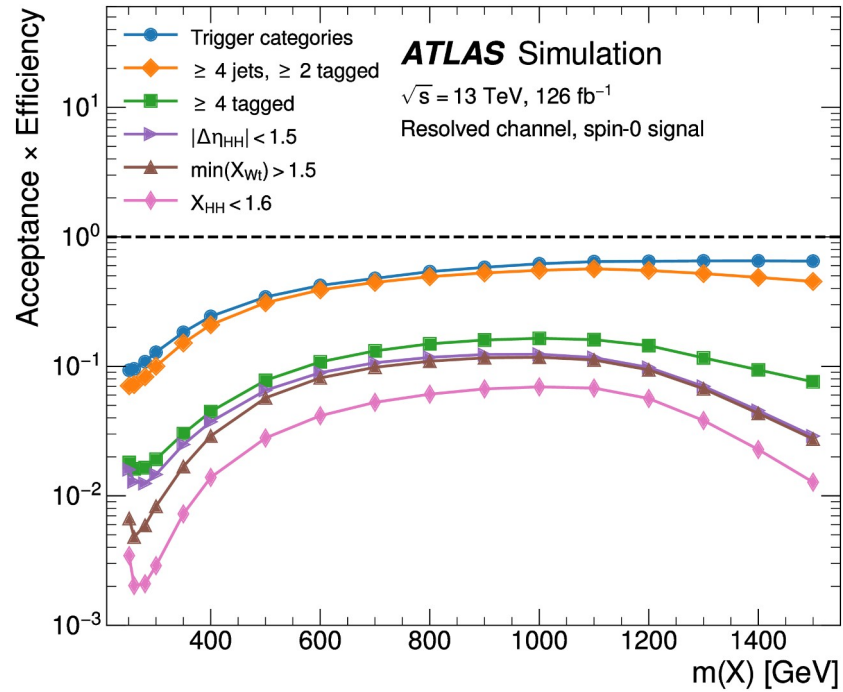
HH→bbbb: Kinematic reweighting inputs

Input features for the neural network that learns the resolved 2b → 4b reweighting:

1. $\log(p_{\mathrm{T}})$ of the selected jet with the second-highest p_{T},

2. $\log(p_{\mathrm{T}})$ of the selected jet with the fourth-highest p_{T},

3. $\log(\Delta R)$ between the two selected jets with the smallest ΔR,

4. $\log(\Delta R)$ between the other two selected jets,

5. the average $|\eta|$ of selected jets,

6. $\log(p_{\mathrm{T}})$ of the HH system,

7. ΔR between the two H candidates,

8. $\Delta\phi$ between the jets making up H_1,

9. $\Delta\phi$ between the jets making up H_2,

10. $\log(\min(X_{Wt}))$, and

11. the number of jets in the event with $p_{\mathrm{T}} > 40\,\mathrm{GeV}$ and $|\eta| < 2.5$, including jets that are not selected.

HH→bbbb: Boosted mass plane
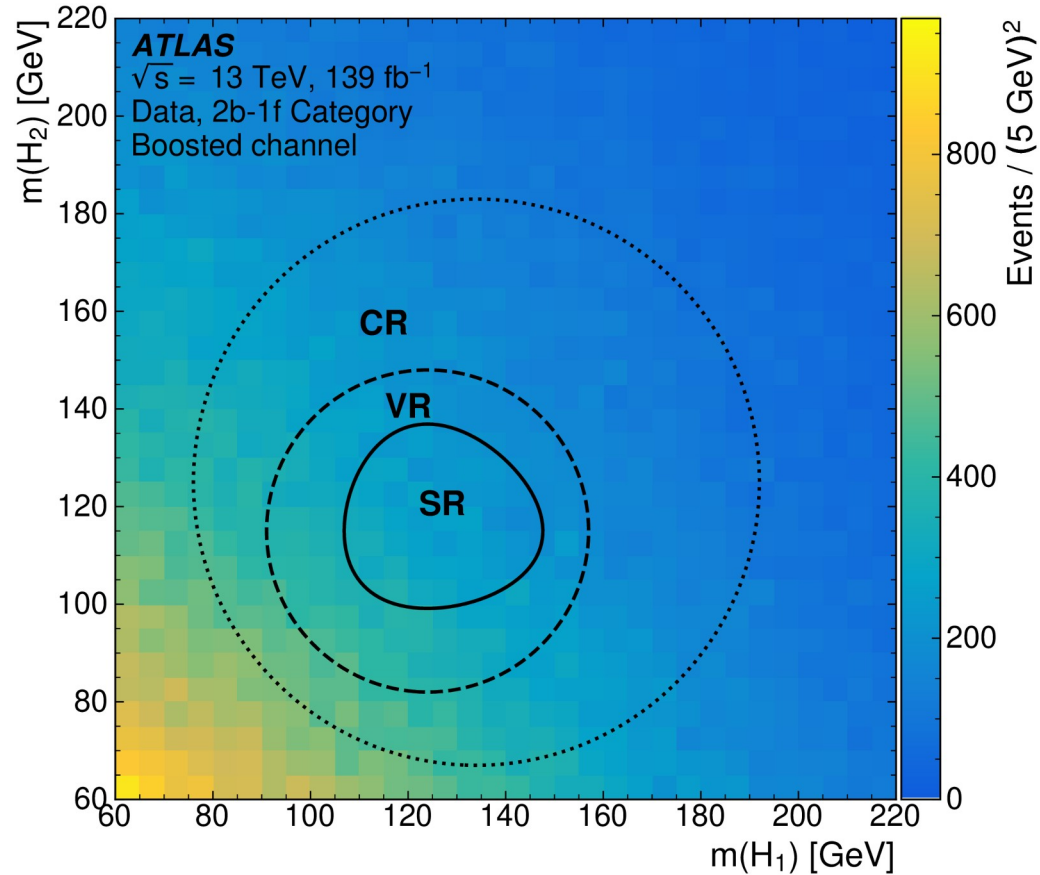
HH→bbbb: Uncertainty Breakdown

Table 6: Impacts of the main systematic uncertainties on the expected 95% CL upper limits on the signal cross-section for four illustrative values of $m(X)$. These are defined as the relative decrease in the expected limit when each relevant nuisance parameter is held fixed to its best-fit value instead of being assigned an uncertainty. The spin-0 signal model is used here.

Uncertainty category	Relative impact [%]			
	280 GeV	600 GeV	1600 GeV	4000 GeV
Background $m(HH)$ shape	12.5	8.7	1.1	1.0
Jet momentum/mass scale	0.6	0.1	1.2	1.7
Jet momentum/mass resolution	2.1	1.5	7.1	7.8
b-tagging calibration	0.7	0.4	2.1	7.0
Theory (signal)	0.6	0.6	1.4	1.2
Theory ($t\bar{t}$ background)	N/A	N/A	0.5	0.2
All systematic uncertainties	15.9	10.9	13.4	15.6